EBioMedicine 61 (2020) 103068

Contents lists available at ScienceDirect

EBioMedicine

journal homepage: www.elsevier.com/locate/ebiom

NDRG2 regulates adherens junction integrity to restrict colitis and tumourigenesis

Mengying Wei[a,1], Yongzheng Ma[a,1], Liangliang Shen[a,1], Yuqiao Xu[b,1], Lijun Liu[a], Xin Bu[a], Zhihao Guo[a], Hongyan Qin[c], Zengshan Li[b], Zhe Wang[b], Kaichun Wu[d], Libo Yao[a], Jipeng Li[e,f,*], Jian Zhang[a,g,**]

[a] The State Key Laboratory of Cancer Biology, Department of Biochemistry and Molecular Biology, the Fourth Military Medical University, Xi'an 710032, China
[b] The State Key Laboratory of Cancer Biology, Department of Pathology, the Fourth Military Medical University, Xi'an 710032, China
[c] State Key Laboratory of Cancer Biology, Department of Medical Genetics and Developmental Biology, Fourth Military Medical University, Xi'an 710032, China
[d] State Key Laboratory of Cancer Biology, Xijing Hospital of Digestive Disease, Xijing Hospital, The Fourth Military Medical University, Xi'an 710032, China
[e] State Key Laboratory of Cancer Biology, National Clinical Research Center for Digestive Diseases and Xijing Hospital of Digestive Diseases, Fourth Military Medical University, 710032 Xi'an, China
[f] Department of Experimental Surgery, Xijing Hospital, Fourth Military Medical University, 710032 Xi'an, China
[g] Key Laboratory of Gastrointestinal Pharmacology of Chinese Materia Medica of the State Administration of Traditional Chinese Medicine, Xi'an 710032, China

ARTICLE INFO

Article History:
Received 25 April 2020
Revised 26 September 2020
Accepted 29 September 2020
Available online xxx

Keywords:
Colitis
NDRG2
Adherens junction
Colitis-associated colorectal cancer

ABSTRACT

Background: Paracellular barriers play an important role in the pathogenesis of Inflammatory bowel disease (IBD) and maintain gut homeostasis. N-myc downstream-regulated gene 2 (NDRG2) has been reported to be a tumour suppressor gene and to inhibit colorectal cancer metastasis. However, whether NDRG2 affects colitis initiation and colitis-associated colorectal cancer is unclear.

Methods: Intestine-specific *Ndrg2* deficiency mice ($Ndrg2^{\Delta IEC}$) were subjected to DSS- or TNBS-induced colitis, and AOM-DSS-induced colitis-associated tumour. HT29 cells, Caco2 cells, primary intestinal epithelial cells (IECs) from $Ndrg2^{\Delta IEC}$ mice, mouse embryo fibroblasts (MEFs) from systemic *Ndrg2* knockout mice, HEK293 cells and human UC and DC specimens were used to investigate NDRG2 function in colitis and colitis-associated tumour.

Findings: Ndrg2 loss led to adherens junction (AJ) structure destruction *via* E-cadherin expression attenuation, resulting in diminished epithelial barrier function and increased intestinal epithelial permeability. Mechanistically, NDRG2 enhanced the interaction of E3 ligase FBXO11 with Snail, the repressor of E-cadherin, to promote Snail degradation by ubiquitination and maintained E-cadherin expression. In human ulcerative colitis patients, reduced NDRG2 expression is positively correlated with severe inflammation.

Interpretation: These findings demonstrate that NDRG2 is an essential colonic epithelial barrier regulator and plays an important role in gut homeostasis maintenance and colitis-associated tumour development.

Funding: National Natural Science Foundation of China (No. 81770523, 31571437, 81672751), Creative Research Groups of China (No. 81421003), State Key Laboratory of Cancer Biology Project (CBSKL2019ZZ11, CBSKL201406, CBSKL2017Z08 and CBSKL2017Z11), Fund for Distinguished Young Scholars of ShaanXi province (2019JC-22).

1. Introduction

Inflammatory bowel disease (IBD) is a multifactorial chronic inflammatory disease mainly comprising Crohn's disease (CD) and ulcerative colitis (UC), which causes intestinal epithelial cell injury and relapsing chronic pathogenic rectal and colonic inflammation [1,2]. Intestinal epithelial homeostasis plays an important role in the

* Corresponding author at: The State Key Laboratory of Cancer Biology, Department of Biochemistry and Molecular Biology, the Fourth Military Medical University, 710032 Xi'an, China.
** Corresponding author at: State Key Laboratory of Cancer Biology, National Clinical Research Center for Digestive Diseases and Xijing Hospital of Digestive Diseases, Fourth Military Medical University, 710032 Xi'an, China.
E-mail addresses: jipengli1974@aliyun.com (J. Li), biozhangj@fmmu.edu.cn (J. Zhang).
[1] These authors contributed equally to this work.

https://doi.org/10.1016/j.ebiom.2020.103068

Research in Context

Evidence before this study

Paracellular barriers such as AJs play an important role in the pathogenesis of IBDs to maintain gut homeostasis. AJ dysfunction is closely associated with IBD, and expression attenuation of the major component E-cadherin could aggravate colitis.

Added value of this study

We demonstrated that intestinal-specific *Ndrg2* knockout led to adherens junction structure destruction via E-cadherin reduction, resulting in diminished epithelial barrier function and enhanced gut permeability, caused mild spontaneous colitis with ageing, and aggravated colitis initiation and colitis-associated tumour development.

Implications of all the available evidence

Our study reveals that NDRG2 is an essential intestinal epithelial barrier regulator and plays important roles in gut homeostasis maintenance and colitis-associated tumour development.

intestinal tract. This bacteria-host homeostasis is maintained by an epithelial barrier, which includes tight junctions (TJs), adherens junctions (Ajs) and desmosomes [3,4]. Ajs are cell-cell adhesion complexes that participate in embryogenesis and tissue homeostasis [5]. The major AJ component E-cadherin or p120-catenin loss results in embryonic death [2]. Previous studies have demonstrated that AJ dysfunction is associated with IBD and that E-cadherin expression attenuation can aggravate colitis, possibly due to an increase in colonic epithelial barrier permeability [6].

We have previously identified N-myc downstream regulated gene 2 (NDRG2) as a novel tumour suppressor gene that plays a role in regulating the proliferation, differentiation and metastasis of multiple types of malignant tumours [7,8]. Notably, our recent data show that NDRG2 can inhibit colorectal cancer cell proliferation and promote cell differentiation [9]. Moreover, we have shown that decreased NDRG2 expression is a powerful and independent predictor of a poor prognosis in colorectal cancer [10,11]. However, whether NDRG2 participates in intestinal epithelial homeostasis and colitis initiation remains unknown.

In this study, we generated intestine-specific conditional *Ndrg2* knockout mice and examined the roles of *Ndrg2* in AJ structure and permeability regulation in the setting of spontaneous and experimentally induced colitis. Furthermore, we characterized the detailed function and mechanism of NDRG2 in intestinal epithelial inflammation and evaluated the effects of *Ndrg2* deficiency on gut inflammation and colitis-associated tumour.

2. Materials and methods

2.1. Mice

Intestine-specific *Ndrg2* knockout mice ($Ndrg2^{\Delta IEC}$) were generated by Shanghai Biomodel Organism Science and Technology Development Co., Ltd., and maintained on a C57BL6/J background. All animals were raised under specific-pathogen-free conditions. The wild-type (WT) and $Ndrg2^{\Delta IEC}$ mice were age-matched, and all the mice that were used in the experiments were male. Typically, at least 8 mice were included each treatment group, and all experiments were repeated at least three times.

2.2. Spontaneous murine colitis analysis

To analyse spontaneous colitis development, 8 weeks and 36 weeks age $Ndrg2^{\Delta IEC}$ mice were first given 1 g/L ampicillin (Sigma-Aldrich, A9393) water for one week, which was then replaced with normal water. The animals were raised under specific-pathogen-free conditions and sacrificed at the indicated time, and colon tissues were collected for further detection. Age-matched WT mice were used as a control. Throughout the experiment, the mice had free access to food and water. The mice were sacrificed in a CO_2 chamber at a low-flow rate of 10-30% volume displacement per minute, followed by cervical dislocation.

2.3. DSS-induced colitis and colitis-associated colorectal cancer

For the DSS-induce colitis model, 8-week-old male mice were treated with 2.5% DSS (w/v, MW 36−50 kDa; MP Biomedicals, Solon, OH, 160110) in their drinking water for 5 days, followed by DSS-free water for another 5 days. Then sacrifice the mice and evaluate the inflammatory responses. Distal colon was obtained for histological analysis, and IECs and LPCs were separated with the total colon.

To induce colitis-associated colorectal cancer, we used the combination of the carcinogen azoxymethane (AOM, MedChemExpress, hy-111375) with repeated treatment with DSS in drinking water. Mice were treated with an intraperitoneal injection of a single dose of AOM (12 mg/kg). After 3 days, 2% DSS dissolved in the drinking water was administered for 6 days (the DSS solution was refreshed on day 3), followed by 15 days of regular drinking water. The DSS treatment was repeated for another two cycles. Mice were sacrificed 100 days after AOM injection, colons were removed and the colon tumours were dissected for further analysis.

2.4. TNBS-induced murine colitis

The 2,4,6-trinitrobenzenesulfonic acid (TNBS, 5%, w/v, Sigma-Aldrich, p2297)-induced experimental colitis was performed in C57BL/6 mice (B6) as previously described. Briefly, $Ndrg2^{\Delta IEC}$ mice and their littermate controls were anaesthetized after fasting for 12 hours, after which 100 μl of 3 mg TNBS (dissolved in 50% ethanol) was slowly instilled into the colon using a 3.5 F catheter, which was inserted intra-rectally 4 cm from the anus. Mice were held in an inverted vertical position for 30 s after instillation to ensure an even distribution of TNBS throughout the entire colon and caecum. Mice from the respective control groups received PBS in a comparable volume via the same route.

2.5. Disease activity index (DAI) scores and Histological score determination

For each mouse, colonic tissue was cut into four segments and fixed in 4% neutral-buffered formalin, embedded in paraffin, cut into 5 μm-thick sections, and stained with H&E. The DAI score was composed of the sum of Diarrhea score (0-solid formed stool, 1-soft stool, and 2- loose formed stool), and rectal bleeding score (0-no blood, 1- the dimly visible streak of blood in stool, 2-gross bleeding from rectum). The histological score was evaluated in a blind manner that consisted of the sum of four parameters ranging from 0−3: cell hyperplasia (0, absent; 1, weak; 2, moderate; and 3, severe); epithelial damage (0, absent; 1, weak; 2, moderate; and 3, severe); inflammatory cell infiltration (0, rare inflammatory cells in lamina propria; 1, increased granulocytes in the lamina propria; 2, confluence of inflammatory cells extending into the submucosa; 3, transmural extension of the infiltrate); and crypt damage (0, intact crypt; 1, loss of basal one-third; 2, loss of basal two-thirds; 3, entire crypt loss; 4, erosion; 5, confluent erosion). The histological score for one mouse

was the average of the summed scores from three biopsies of each of the four colon segments.

2.6. Isolation of intestinal epithelial cells (IECs) and lamina propria cells (LPCs)

Mice were sacrificed, and total colon tissues were dissected, opened longitudinally and washed extensively in cold PBS. The colon tissue was cut into 1 cm segments, which were washed with fresh PBS. The tissues were incubated with digestion buffer containing 8 mM EDTA (Sigma-Aldrich, E9884) and 1 mM DTT (Roche, 10197777001) at 37 °C for 20 min, which was then replaced with digestion buffer with cold PBS and shaken vigorously for 1 min. The process was repeated once. The supernatants were combined and centrifuged at 2000 rpm for 5 min at 4 °C. The pelleted cells were digested with dispase Ⅱ (0.2 mg/ml, Roche, 04942078001) in PBS at 37 °C for 5 min. The suspension was filtered with 70 μm and 40 μm nylon filters (BD biosciences) and centrifuged at 2000 rpm for 5 min at 4 °C, after which the cells were resuspended in cold PBS. To obtain LPCs, tissues incubated with EDTA were cut into small pieces and digested with a mixture of collagenase A (2 mg/ml, Roche, 10103586001) and DNase I (0.05 mg/ml, Sigma, D4263) in PBS at 37 °C for 35 min. After incubation, the enzyme mixture was replaced with cold PBS and shaken for 2 min. The process was repeated once. The suspension was combined and passaged through 70 μm and 40 μm nylon filters, followed by centrifugation at 4000 rpm for 5 min at 4 °C and resuspension of the pelleted cells in cold PBS. IECs were used for extraction of RNA and Western blot analysis. For quantification of immune cells, both IECS and LPCs were combined and used for subsequent FACS analysis immediately.

2.7. Analysis of intestinal permeability

Fluorescein isothiocyanate-conjugated (FITC) dextran with an average mol wt of 40,000 (Sigma-Aldrich, FD40) or an average mol wt of 500,000 (Sigma-Aldrich, FD500S) was dissolved at a concentration of 100 mg/ml in PBS. According to the manufacturer's instructions, all experimental mice were treated with water starvation for at least 10 hours; then, FITC-dextran was administered to each mouse (44 mg/100 g body weight) by oral gavage with a needle attached to a 1-ml syringe. After 4 hours, from mice anaesthetized was collected at least 400 μl of blood per mouse. Serum was separated and collected according to the manufacturer's instructions and stored in the dark at 4 °C. One hundred fifty microlitres of serum with an equal volume of PBS and 100 μl of the dilution were added to a 96-well microplate in duplicate. The concentration of FITC-dextran was determined using a spectrophotometry fluorometer (Tecan GENios Microplate Reader) with an excitation of 485 nm (20-nm band width) and an emission wavelength of 528 nm (20-nm band width). Serum from untreated mice was used to determine the background.

2.8. Flow cytometry staining

For the detection of monocytes, macrophages and neutrophils, the following fluorochrome-conjugated antibodies were used: anti-mouse CD11b FITC (eBioscience, 11-0112, AB_464933), anti-mouse Ly-6G (Gr-1) PE (eBioscience, 12-5931, AB_466045), anti-mouse F4/80 Antigen APC (eBioscience, 17-4801, AB_469452), and PE rat anti-mouse Siglec-F (BD Pharmingen™ 562068, AB_10896143). According to the reported methods, CD11b staining was used to detect monocytes, the combination of CD11b and Ly-6G (Gr-1) was used to detect neutrophils, and the combination of CD11b and Siglec-F was used to quantify eosinophils, while macrophages were detected with CD11b and F4/80. Both IECs and LPCs were combined for quantification of the immune cells. Total cells were resuspended in PBS containing 5% FBS, and at least 10^6 cells were used for the staining.

2.9. Analysis of adherens junction by transmission electron microscopy

Mice were perfused through the left atrium with a mixture of 4% paraformaldehyde (Servicebio, G1101) and 1% glutaraldehyde (Sigma-Aldrich, G5882). Pieces of colon tissue were fixed in 3% glutaraldehyde with 2% OsO4 (Sigma-Aldrich, 75633) for 6 hrs at 4 °C. The tissue was dehydrated at 4 °C through a series of acetone concentrations (50, 70, 90, 96, 100%) and embedded in Epon 812 epoxy resin (all from Epoxy Embedding Medium kit, Sigma-Aldrich, 45359). Sections were cut to a thickness of 70 nm and collected on 200-mesh, Formvar-coated copper grids. The grids were stained with uranyl acetate and lead citrate (both from Sigma-Aldrich, 45359), and micrographs were collected with a JEOL JEM 1230 electron microscope (JEOL, Japan).

2.10. RNA isolation and quantitative real-time PCR (qPCR)

Total IEC RNA was isolated from healthy and DSS-treated WT and *Ndrg2*$^{\Delta IEC}$ mice using TRIzol reagent (Takara, Dalian, China, T9108) according to the manufacturer's instructions. Primer sequences for quantitative real-time polymerase chain reaction (qRT-PCR) are listed in Supplementary Tables 1 and 2. qRT-PCR data were analysed by the $2^{-\Delta\Delta CT}$ method, with *GAPDH* and β-actin as the housekeeping gene.

2.11. Co-immunoprecipitation assay

FLAG-tagged NDRG2 plasmids (full-length and truncated form named NDRG2/FL, NDRG2/ΔN, and NDRG2/ΔC) were co-transfected with Myc-Snail, HA-FBXO11 (gift from Dr. Yibin Kang, Princeton University) and V5-Ubiquitin or the indicated plasmids as described in the figures in 60-mm dishes using Lipofectamine™ 2000 Transfection Reagent (Invitrogen™, 11668019) according to the manufacturer's instructions. For the ubiquitination assay, cells were treated with 10 μM MG132 (Sigma-Aldrich, M8699) for the indicated times after 2 days of transfection. The cells were then harvested with lysis buffer (Beyotime, P0013), and the proteins were quantified using the Pierce BCA Protein Assay Kit (Thermo Scientific, 23225) and adjusted to equal concentrations. Cell lysates were then immunoprecipitated with primary anti-FLAG (Sigma-Aldrich, F1804, AB_262044) or anti-Myc (Cell Signaling, 66004, AB_1549585) or anti-HA (CST, 3724, AB_1549585) or anti-V5 (Sigma, V8137) at 4 °C overnight. Then, 70 μL protein A/G sepharose (Abcam, ab193262) was added and incubated for 3 hrs. After 3 washes using NETN wash buffer, Tris 20 mM (pH 8.0), NaCl 100 mM, EDTA 1 mM, NP-40 0.5%, and sepharose beads were collected and re-suspended in 70 μL 2× SDS buffer. The samples pulled down with 5% input were resolved on SDS-PAGE gels and transferred to NC membranes. Then, the membranes were detected with appropriate antibodies and visualized using a Tanon 6200 Luminescent Imaging Workstation.

2.12. Western blot analysis

Total proteins were extracted from intestinal epithelial cells (IECs) according to the manufacturer's recommendations. Sodium dodecyl sulfate polyacrylamide gel electrophoresis (SDS-PAGE) and Western blot analysis were performed with 40 μg protein. The following antibodies were used: β-actin (Cell Signaling, 12262, AB_2566811), NDRG2 (Cell Signaling, 5667, AB_10829238), E-cadherin (Cell Signaling, 3195, AB_2291471), β-catenin (Cell Signaling, 8480, AB_11127855), P120 catenin (Proteintech, 12180, AB_2086267), α-catenin (Cell Signaling, 13-9700), Snail (Cell Signaling, 3879,

AB_2255011), Slug (Cell Signaling, 9585, AB_2239535), and Claudin-1 (Cell Signaling, 13255, AB_2798163).

2.13. Immunofluorescence staining

For the murine studies, 8-μm frozen segments of colon from WT and ΔIEC mice were fixed in cold acetone for 15 min at −20 °C, and then 3% BSA was used for blocking at 25 °C for 1 h. Anti-E-cadherin (1:100), NDRG2 (1:80), β-catenin (1:100), P120 catenin (1:100) and ZO-1 (Cell Signaling, 8193, AB_10898025, 1:100) was used for incubation at 4 °C overnight, and Alexa-Fluor 488- or 647- conjugated antibody (Invitrogen, AB_2633280, AB_2633282, 1:2000) was used as the secondary antibody and incubated for 1 h at 25 °C. Incubation with 1 μg/ml of DAPI was performed for 15 min. Fluorescence analysis was performed with a laser scanning confocal microscope A1 (Nikon). For cellular protein distribution detection, cells were seeded in rat tail collagen-coated dishes and transfected with the indicated plasmid for 24 h, followed by gentle washing with PBS for 5 min and fixation in 4% paraformaldehyde for 30 min. Immunofluorescence staining was performed according to the above-described method. Anti-HA (1:500), anti-FLAG (1:500) and anti-SNAIL (1:200) were used for incubation at 4 °C overnight.

2.14. Membrane protein extraction

Membrane proteins were separated using a Mem-PER™ Plus Membrane Protein Extraction Kit (Thermo Scientific™, 89842) according to the manufacturer's instructions. Briefly, freshly isolated IECs from both *Ndrg2*$^{\Delta IEC}$ mice and WT mice were washed with PBS and centrifuged at 300 × g for 5 min. The cell pellet was washed with 3 mL of Cell Wash Solution and centrifuged at 300 × g for 5 min. Then, the supernatant was discarded, and the cells were resuspend in 1.5 mL of Cell Wash Solution, centrifuged at 300 × g for 5 min and the supernatant discarded. We added 0.75 mL of Permeabilization Buffer to the cell pellet, vortexed it briefly and incubate it for 10 min at 4 °C with constant mixing. The permeabilized cells were centrifuged for 15 min at 16,000 × g. The supernatant containing cytosolic proteins was removed and transferred to a new tube. Then, 0.5 mL of Solubilization Buffer was added to the pellet, and the cells were suspended. The tubes were incubated at 4 °C for 30 min with constant mixing and centrifuged at 16,000 × g for 15 min at 4 °C. The supernatant containing solubilized membrane and membrane-associated proteins was transferred to a new tube. Both membrane and cytoplasm fractions could be used immediately or stored at −80 °C for future use.

2.15. Tissue samples and immunohistochemistry staining

A total of 19 ulcerative colitis cases and 5 Crohn's disease patient samples were obtained from Xijing Hospital from April 2013 to October 2016. These paraffin-embedded tissues were sectioned at 4-μm thickness and stained with HE or the indicated antibody using standard immunohistochemistry methods. The clinical information is shown in Supplementary Table 3.

2.16. Study approval and ethics statement

All animal procedures and patients sample study were reviewed and approved by the Animal Care and Ethic Committee of Fourth Military Medical University (No. KY20173182-1). All animals were housed, cared for, and used in compliance with the guidelines regarding the humane use and care of laboratory animals for biomedical research published by the National Institutes of Health (No. 85-23, revised 1996). All patients in the disease sample cohort provided full consent for the study.

2.17. Statistical analysis

Differences in parametric data were evaluated using the Student's t test or one-way analysis of variance (ANOVA). $^{*}p<0.05$ and $^{**}p<0.01$ were considered statistically significant.

3. Results

3.1. Intestinal Ndrg2 knockout mice develop mild spontaneous colitis

To determine the role of NDRG2 in colitis initiation, we generated intestine-specific conditional *Ndrg2* knockout mice featuring intestinal epithelial cells lacking *Ndrg2* (Supplementary Fig. 1(a)). NDRG2 expression was specifically and completely abolished in the intestinal epithelial cells (IECs) of *Ndrg2*$^{\Delta IEC}$ mice (Supplementary Fig. 1(b), (c)). The mice were kept under specific-pathogen-free (SPF) conditions, and their body weight was monitored each week. Intriguingly, we observed significant growth retardation of *Ndrg2*$^{\Delta IEC}$ mice compared with the wild type (WT) group, especially after 16 weeks age (Fig. 1(a)). However, there was no significant difference in the activity and diet between the two groups of mice. Thus, it was crucial for us to detect the alteration of intestinal tissues. As shown by the haematoxylin eosin (H&E) staining data in Fig. 1(b)–(c), increased intestinal inflammation was observed in *Ndrg2*$^{\Delta IEC}$ mice that became more severe with ageing, which indicated the spontaneous colitis in *Ndrg2*$^{\Delta IEC}$ mice.

Next, to confirm that the growth retardation of *Ndrg2*$^{\Delta IEC}$ mice was mainly due to increased intestinal inflammation, we treated the WT and *Ndrg2*$^{\Delta IEC}$ mice (8 weeks age) with ampicillin (1 g/L) water for one week to alleviate any potential inflammation in digestive tract, and partially synchronize the gastrointestinal tract conditions between wild type and *Ndrg2*$^{\Delta IEC}$ mice without disturbing weight and food intake, as mild intestinal inflammation might occurred during mice feeding under SPF condition and ampicillin is a broad-spectrum antibiotic that can effectively remove gram-positive and gram-negative bacteria (the major source of LPS) [12,13]. Then, we monitored the body weight in each group (Fig. 1(d)), as anticipated, there was a noticeable slower increase in body weight in the *Ndrg2*$^{\Delta IEC}$ mice compared with the WT group (Fig. 1(e)). Additionally, more severe intestinal inflammation and increased IL-1β and IL-6 expression were observed in the *Ndrg2*$^{\Delta IEC}$ mice (Fig. 1(f)–(h)), further supporting the increased spontaneous colitis in these mice. Then, we used the old age mice to further confirm this observation. As shown in Fig. 1(i), both the WT and *Ndrg2*$^{\Delta IEC}$ mice aged 36 weeks were treated with ampicillin for 1 week and their body weight and intestinal inflammation analysed after 12 weeks, respectively. Compared with the increased body weight of WT mice after 12 weeks, there was no significant alteration of *Ndrg2*$^{\Delta IEC}$ mice (Fig. 1(j)). Similar to the findings in young mice (Fig. 1(f)–(h)), increased intestinal inflammation and IL-1β and IL-6 expression were detected in the *Ndrg2*$^{\Delta IEC}$ mice (Fig. 1(k)–(m)). Collectively, these data strongly suggested that intestinal *Ndrg2* knockout facilitated the development of mild spontaneous colitis.

3.2. Intestinal Ndrg2 loss aggravates chemical-induced colitis

To further determine the role of NDRG2 in colitis initiation and progression, we treated the mice with DSS (dextran sodium sulphate) and TNBS (2,4,6-trinitrobenzenesulfonic acid), respectively, to mimic the colitis in vivo. We found that intestinal *Ndrg2*$^{\Delta IEC}$ mice exhibited an increased body weight loss compared with WT mice with DSS treatment (Fig. 2(a)), as well as more severe colonic shortening than their counterparts (Fig. 2(b) and (c)). For histological analysis, *Ndrg2*$^{\Delta IEC}$ mice exhibited severe colitis characterized by profound epithelial structural damage and robust inflammatory cell infiltration than the WT group (Fig. 2(d) and (e)), as well as higher disease

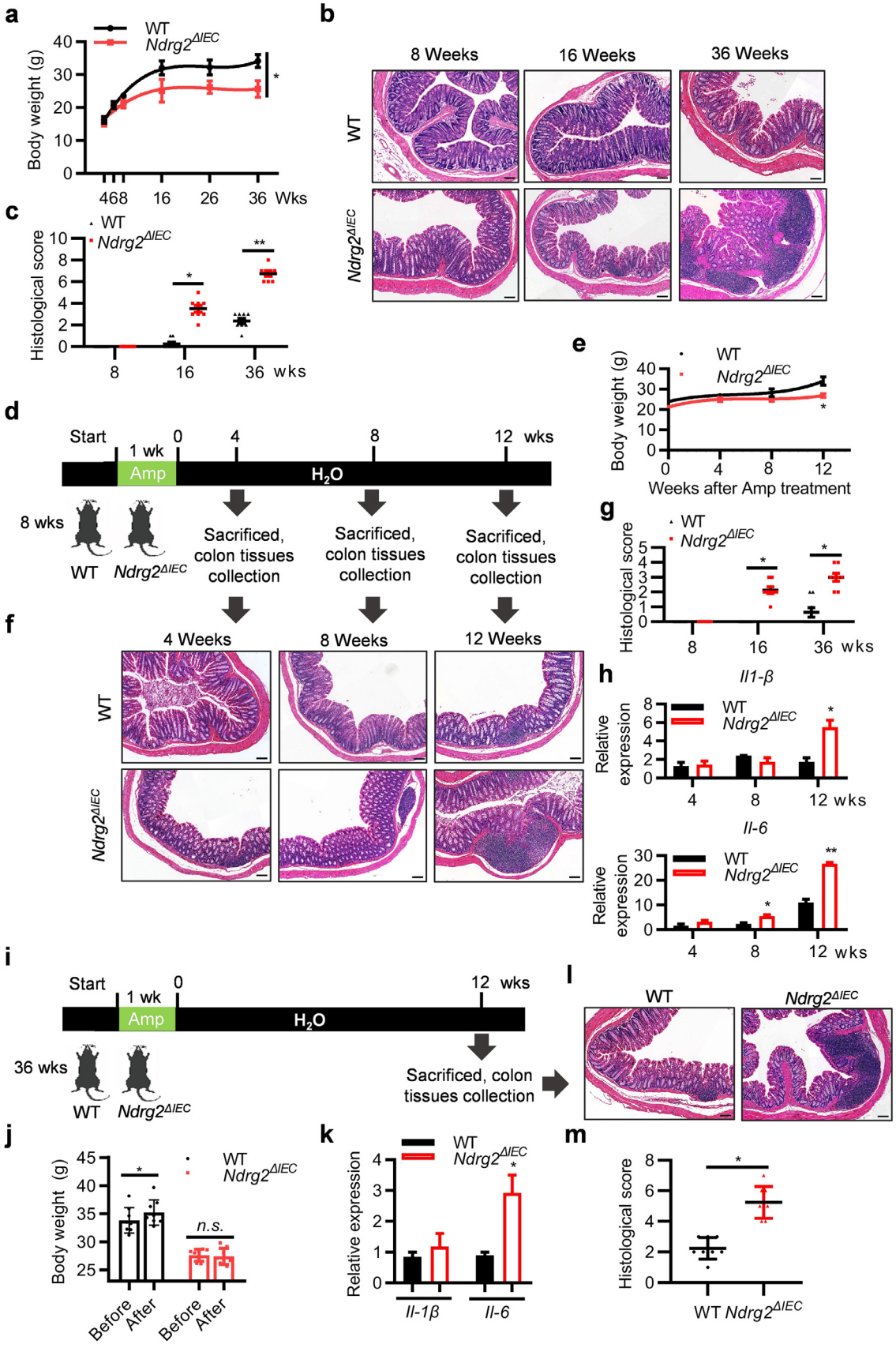

Fig. 1. Intestine-specific conditional *Ndrg2* knockout mice (*Ndrg2*$^{\Delta IEC}$) spontaneously developed into mild colitis with ageing. (a) Body weight of WT and *Ndrg2*$^{\Delta IEC}$ mice at the indicated time with specific-pathogen-free (SPF) feeding conditions (n=8/group; $^{*}p<0.05$, (Student's t test)). **(b) and (c)** Histological score and H&E-staining of colon section from WT and *Ndrg2*$^{\Delta IEC}$ mice of the indicated ages. Representative data of 3 independent experiments. Scale bar: 100 μm. **(d)** Schematic diagram to analyse the occurrence of spontaneous colitis in 8-week-old WT and *Ndrg2*$^{\Delta IEC}$ mice after withdrawal of ampicillin treatment for 1 week. **(e)** Body weight of WT and *Ndrg2*$^{\Delta IEC}$ mice at the indicated time after ampicillin withdrawal (n=8/group; $^{*}p<0.05$, (Student's t test)). **(f) and (g)** Histological score and H&E-staining of colon tissue. Representative data of 3 independent experiments.

activity index (DAI) scores (Fig. 2(f)). Alternatively, we observed similar results with more severe inflammation of *Ndrg2*$^{\Delta IEC}$ mice in the TNBS-induced colitis model (Supplementary Fig. 2(a), (b)). For the survival analysis, *Ndrg2*$^{\Delta IEC}$ mice exhibited increased susceptibility to lethal colitis induction (4% DSS for 7 days), leading to a shorter survival compared with WT mice (Fig. 2(g)). Taken together, our data demonstrated that intestine-specific *Ndrg2* deficiency obviously aggravated chemical-induced colitis.

3.3. *Intestinal* Ndrg*2 deficiency promotes inflammatory cell infiltration, chemokine and cytokine expression and LPS permeability*

Inflammatory cell infiltration plays an important role in both UC and CD [14]. To characterize the role of NDRG2 in colonic inflammation, IECs and lamina propria cells (LPCs) were isolated from WT and *Ndrg2*$^{\Delta IEC}$ mice treated with or without 2.5% DSS. Flow cytometry analysis showed that *Ndrg2*$^{\Delta IEC}$ mice exhibited slight increases in monocyte and macrophage infiltration compared with WT mice under the DSS-free condition (Fig. 3(a), Supplementary Fig. 3(a)). Notably, *Ndrg2*$^{\Delta IEC}$ mice exhibited significantly increased monocyte, macrophage and neutrophil infiltration with DSS treatment compared with WT mice (Fig. 3(b), supplementary Fig. 3(a)). Furthermore, DSS-treated *Ndrg2*$^{\Delta IEC}$ mice exhibited dramatically increased chemokine expression of *Cxl5* and *Cxcl1/2*, as well as pro-inflammatory cytokine expression of *Il-1β, Tnf-α* and *Il-6* (Fig. 3(c), Supplementary Fig. 3 (b)). In contrast, mRNA expression of the anti-inflammatory cytokine *IL-10* was attenuated in DSS-treated *Ndrg2*$^{\Delta IEC}$ mice (Fig. 3(c)), while the expression of *Tgf-β, Il-12, Il-17 and Il-22* was comparable between the two groups (Supplementary Fig. 3(b)). These findings indicated that intestinal *Ndrg2* deficiency aggravated DSS-induced colitis by increasing chemokine and pro-inflammatory cytokine expression and promoting inflammatory cell infiltration.

The gut microbiota plays important roles in the pathogenesis of IBD, and lipopolysaccharide (LPS) is the main microflora-derived toxin that induces gut epithelial inflammation. Noticeably, the serum LPS concentration is dramatically increased in IBD patients [15]. As shown in Fig. 3(D), DSS-treated *Ndrg2*$^{\Delta IEC}$ mice exhibited increased serum LPS levels compared with WT mice. Thus, we subsequently examined whether *Ndrg2* deficiency facilitated LPS-induced inflammation. As expected, LPS induced significant inflammation characterized by dose-dependent increases in the levels of *Il-1β*, *Il-6*, *Tnf-α* and *Cxcl1/2* expression (Supplementary Fig. 4(a)–(e)). Additionally, *Ndrg2*$^{\Delta IEC}$ mice exhibited markedly higher LPS permeability and increased *Il-1β*, *Il-6*, *Tnf-α*, and *Cxcl-1/2* expression (Fig. 3(e) and (f)), suggesting an enhanced inflammatory response. These data suggested that intestine-specific *Ndrg2* deficiency increased LPS permeability and promoted LPS-induced inflammation and colitis progression.

3.4. *Intestinal* Ndrg*2 loss disrupts adherens junction integrity of normal epithelium and increases colonic permeability*

Epithelial barrier dysfunction increased gut permeability and aggravated the inflammatory response in IBD. To further investigate the role of *Ndrg2* in DSS-induced colitis, we examined the gut permeability in WT and *Ndrg2*$^{\Delta IEC}$ mice treated with or without DSS *via* FITC-dextran analysis. As shown in Fig. 4(a), even with DSS-free treatment, *Ndrg2*$^{\Delta IEC}$ mice exhibited slightly increased permeability of low molecular weight dextran. As expected, DSS-treated *Ndrg2*$^{\Delta IEC}$ mice showed extremely increased permeability of both low- and high-molecular-weight dextran, strongly suggesting epithelial barrier dysfunction in *Ndrg2*$^{\Delta IEC}$ mice. Structural disruption of the adherens junction (AJ) and tight junction (TJ) resulted in epithelial barrier dysfunction, increased epithelial permeability and inflammation [16,17]. Next, it was very important for us to analyse the epithelial barrier structure difference between WT and *Ndrg2*$^{\Delta IEC}$ mice. Using electron microscopy analysis, we noticed that *Ndrg2*$^{\Delta IEC}$ mice exhibited significant AJ structural disruption but virtually no TJ structural alteration compared with WT mice (Fig. 4(b)). The widths of the AJs were markedly increased in the intestinal epithelium of *Ndrg2*$^{\Delta IEC}$ mice (Fig. 4(c)), indicating intestinal epithelial AJ structure destruction in *Ndrg2*$^{\Delta IEC}$ mice.

The core components of AJ include E-cadherin and the catenin family members p120-catenin, β-catenin and α-catenin [18]. We are eager to understand the causes of the AJ destruction in the *Ndrg2*$^{\Delta IEC}$ epithelium. As shown in Fig. 4(D), there was no obvious alteration of p120-catenin, β-catenin and α-catenin expression in *Ndrg2*$^{\Delta IEC}$ mice (Fig. 4(d)). However, intestinal *Ndrg2* loss caused a dramatic decrease in E-cadherin both in the protein and mRNA levels (Fig. 4(d) and (e)), suggesting the transcriptional regulation of E-cadherin by NDRG2. Beyond localization on AJs, cadherin and catenin family can be released from the cell membrane, undergo re-localization and function in the cytoplasm or nucleus in restricted cellular or developmental contexts. Consistent with the above results, we found that only E-cadherin was markedly decreased in the membrane component (without relocation in other cell compartment) of IECs from *Ndrg2*$^{\Delta IEC}$ mice (Supplementary Figs 5 and 6). Moreover, there was no significant difference in the expression and distribution of ZO-1 (key component of TJs) (Supplementary Figs 5 and 6). Coincidently, the immunofluorescence analysis showed that E-cadherin was significantly decreased in the colonic epithelium of *Ndrg2*$^{\Delta IEC}$ mice (Fig. 4 (f)), suggesting that *Ndrg2* loss resulted in E-cadherin downregulation in vivo. Remarkably, E-cadherin attenuation in *Ndrg2*$^{\Delta IEC}$ mice was much more dramatic following spontaneous colitis with ageing (Supplementary Fig. 7(a) and (b)). These findings demonstrated that *Ndrg2* deficiency disrupts AJ structural integrity in the colonic epithelium, most likely by suppressing E-cadherin expression, thus increasing colonic permeability and inflammation.

3.5. *NDRG2 augments E-cadherin expression by promoting the ubiquitylation and degradation of Snail*

The aforementioned results prompted us to uncover how *Ndrg2* loss caused the transcriptional repression of E-cadherin. However, current studies do not support the concept of NDRG2 as a transcriptional regulator per se [9,19,20]. It is reasonable for us to further analyse whether *Ndrg2* deficiency alters the expression of key transcriptional regulators of E-cadherin, such as Snail, Slug and ZEB1/2, among others [21,22]. Notably, Snail was one of the most changed regulators and increased significantly in *Ndrg2*-deficient IECs and mouse embryonic fibroblast (MEF) cells (Fig. 5(a)). We further confirmed the alteration of SNAIL and E-Cadherin in human colorectal cancer cells with NDRG2 knockdown (Supplementary Fig. 8(a), (b)). Next, by subjecting different FLAG-tagged NDRG2 truncations (Fig. 5 (b), right panel) [9], we found that SNAIL expression was significantly decreased with full-length NDRG2 (NDRG2/FL) but abolished by NDRG2 N-terminal deletion (NDRG2/ΔN) (Fig. 5(b), left panel), suggesting a key role of N-terminal of NDRG2 for SNAIL regulation. With the chase assay of protein stability, we noticed that NDRG2/FL could markedly shorten the half-life of SNAIL protein (Fig. 5(c), (d)). In

Scale bar: 100 μm. **(h)** Quantitative real-time PCR (qRT-PCR) for *Il-1β* and *Il-6* in IECs from WT and *Ndrg2*$^{\Delta IEC}$ mice (n=8/group; $^{*}p<0.05$, $^{**}p<0.01$, (Student's t test)). **(i)** Schematic diagram to analyse the occurrence of spontaneous colitis in 36-week-old WT and *Ndrg2*$^{\Delta IEC}$ mice after withdrawal of ampicillin treatment for 1 week. **(j)** Body weight of 36-week-old WT and *Ndrg2*$^{\Delta IEC}$ mice before and after ampicillin withdrawal (48 weeks age)-induced spontaneous colitis (n=8/group; $^{*}p<0.05$, (Student's t test)). **(k)** qRT-PCR for *Il-1β* and *Il-6* in IECs of (G) (n=8/group; $^{*}p<0.05$, (Student's t test)). **(l) and (m)** Histological score and H&E-staining of colon sections of WT and *Ndrg2*$^{\Delta IEC}$ mice at the indicated times. Representative data of 3 independent experiments. Scale bar: 100 μm.

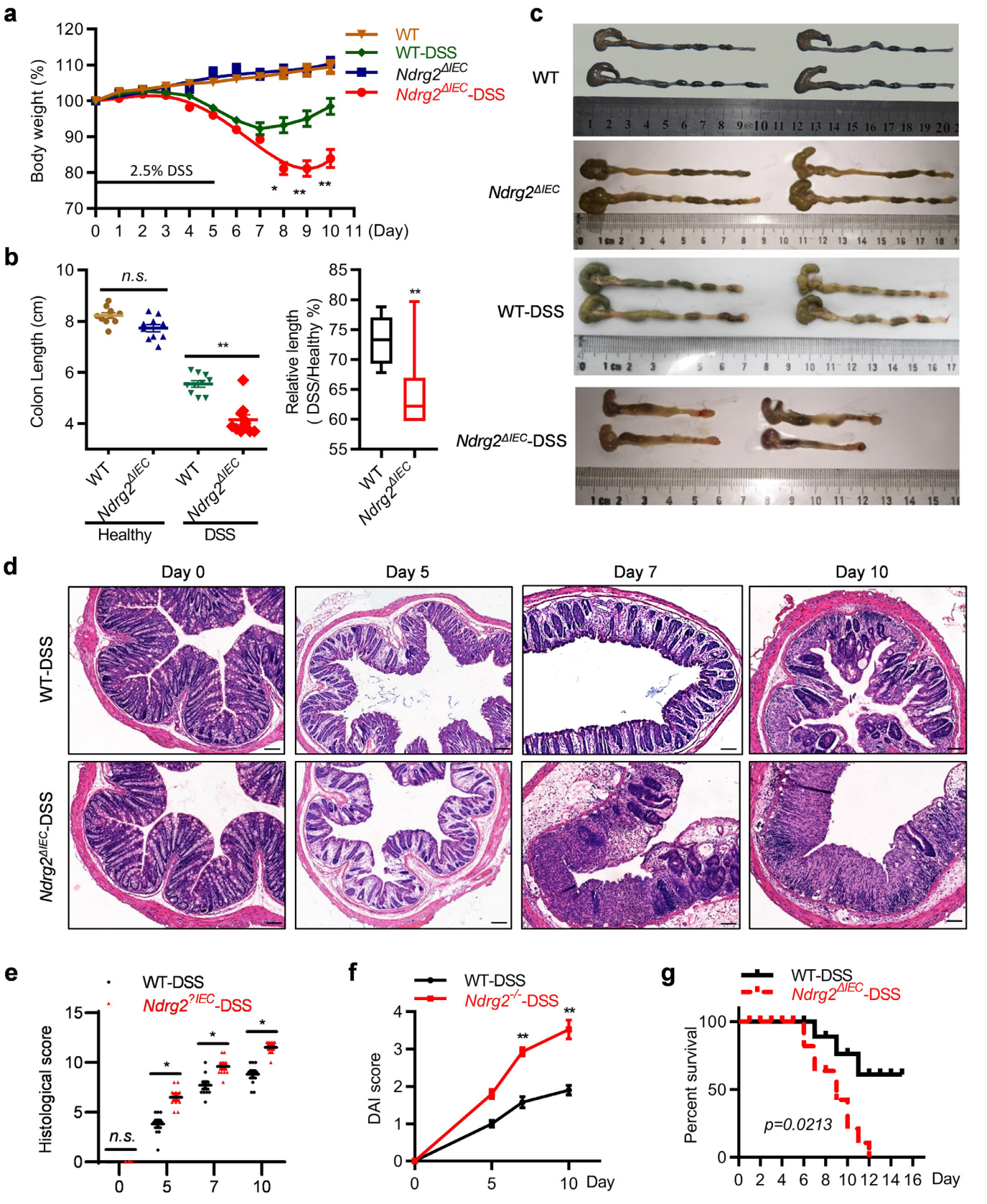

Fig. 2. ***Ndrg2*$^{\Delta IEC}$ mice exhibited increased intestinal susceptibility to dextran sodium sulfate (DSS)-induced colitis.** **(a)** Body weight change of 8-week-old WT and *Ndrg2*$^{\Delta IEC}$ mice with 2.5% DSS treatment (n=10/group; $^{*}p<0.05$, $^{**}p<0.01$, (Student's t test)). **(b)** Colon lengths (left) and statistical results (right) on day 10 in the WT and *Ndrg2*$^{\Delta IEC}$ mice (n=10/group; $^{**}p<0.01$, (Student's t test)). **(d)** Representative images of the colon appearance at the end of the experiments. (n=10/group) **(d)** Representative H&E-staining of colon tissue. (n=10/group). Scale bar: 100 μm. **(e)** The histological scores of the WT and *Ndrg2*$^{\Delta IEC}$ mice on days 0, 5, 7 and 10 of 2.5% DSS administration. (n=6/group; $^{*}p<0.05$, *n.s.*, no significance, (Student's t test)) **(f)** The DAI scores of the WT and *Ndrg2*$^{\Delta IEC}$ mice on days 0, 5, 7 and 10 of 2.5% DSS administration. (n=6/group, $^{*}p<0.05$, $^{**}p<0.01$, (Student's t test)). **(g)** Survival rate analysis of 4% DSS-induced lethal colitis (n=15/group).

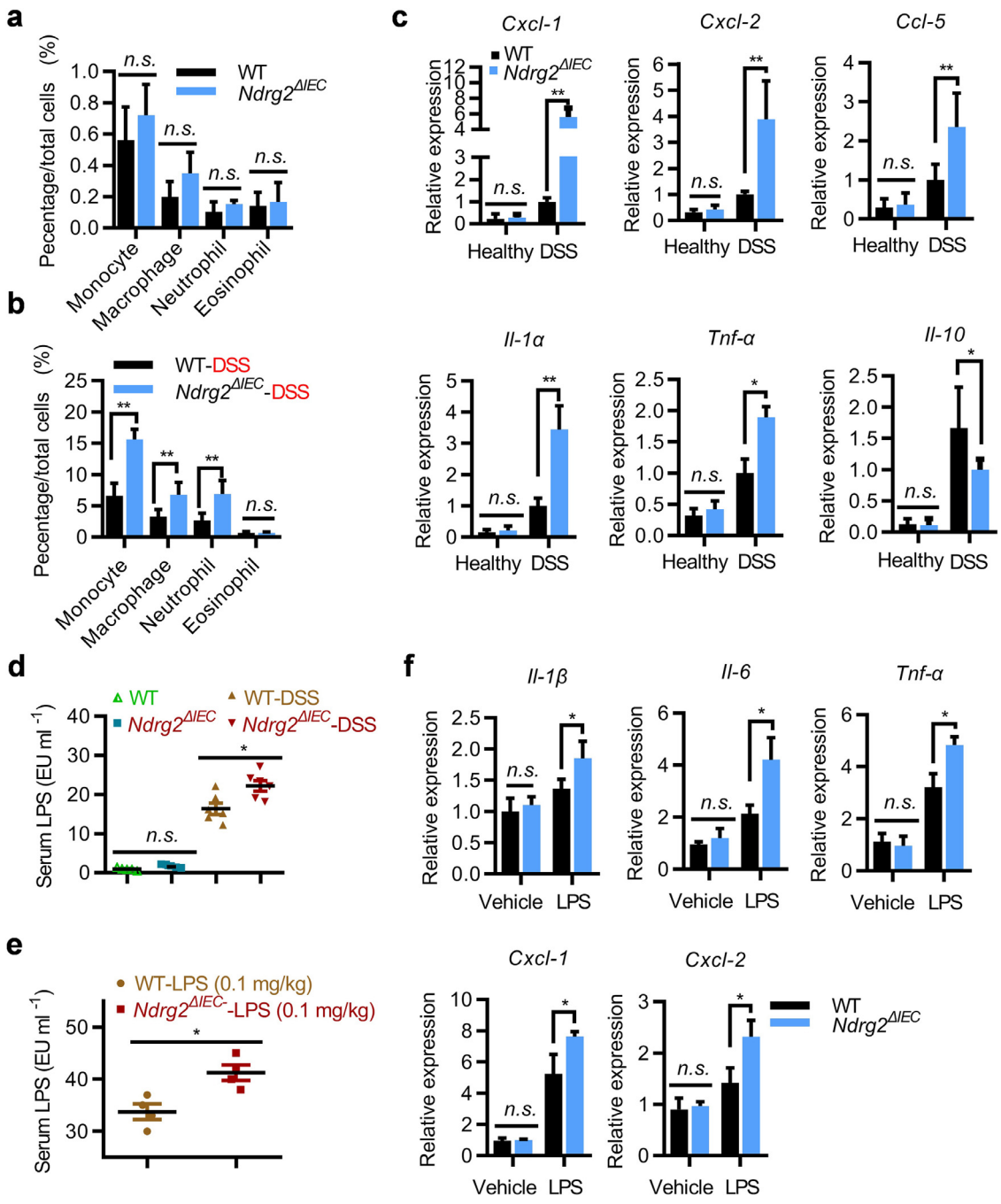

Fig. 3. ***Ndrg2*** **deficiency enhanced inflammation in colon characterized by increased inflammatory cell infiltration and LPS permeability**. WT and *Ndrg2*$^{\Delta IEC}$ mice were treated with 2.5% DSS (n=12/group). Quantification of the infiltrated immunocytes on day 0 **(a)** and day 10 **(b)** detected by flow cytometry analysis. **(c)** qRT-PCR analysis of the chemokines *Cxcl-1, Cxcl-2, Ccl-5* and pro-inflammatory cytokines *Il-1β* and *Tnf-α*, and the anti-inflammatory cytokines *Il-10*. **(d)** Detection of serum LPS concentrations in WT and *Ndrg2*$^{\Delta IEC}$ mice with and without 2.5% DSS treatment (n=6/group). **(e)** Detection of serum LPS levels in WT and *Ndrg2*$^{\Delta IEC}$ mice with 0.1 mg/kg LPS treatment with intrarectal administration after ampicillin treatment for 5 days, (n=4/group). **(f)** qRT-PCR analysis of *Il-1β, Il-6, Tnf-α, Cxcl-1 and Cxcl-2* expression in IECs of WT and *Ndrg2*$^{\Delta IEC}$ mice treated with 0.1 mg/kg LPS (n=4/group). **(a), (b), (c), (d), (e), (f)** Representative data of 3 independent experiments. Data are represented as the mean ± SEM. $^{*}p<0.05$, $^{**}p<0.01$, *n.s.*, no significance (Student's *t* test).

contrast, the protein stability of Snail was significantly increased in *Ndrg2*-deficient MEF cells (Fig. 5(e)). However, SNAIL suppression by NDRG2 was almost completely reversed by the proteasome inhibitor MG132 (Fig. 5(f)), strongly supporting that NDRG2 might promote Snail protein degradation through the ubiquitin-proteasome pathway.

Several reported E3 ligases are responsible for Snail ubiquitylation, including β-TRCP1/Fbxw1, Fbxo11, Fbxl14 and Fbxl5 [23,24]. Thus, we were curious to determine the E3 ligase responsible for Snail ubiquitylation mediated by NDRG2. We used an siRNA strategy to knockdown each of the E3 ligases and compared the protein stability of Snail in NDRG2 overexpression cells (data not shown). Remarkably, siRNA targeting of FBXO11 could significantly rescue the Snail protein stability inhibited by NDRG2 (Fig. 5(g), Supplementary Fig. 9). Based on this finding, we hypothesized that NDRG2 could enhance the interaction of FBXO11 and Snail to promote the ubiquitylation and degradation of Snail. The immunofluorescence assay demonstrated the cellular

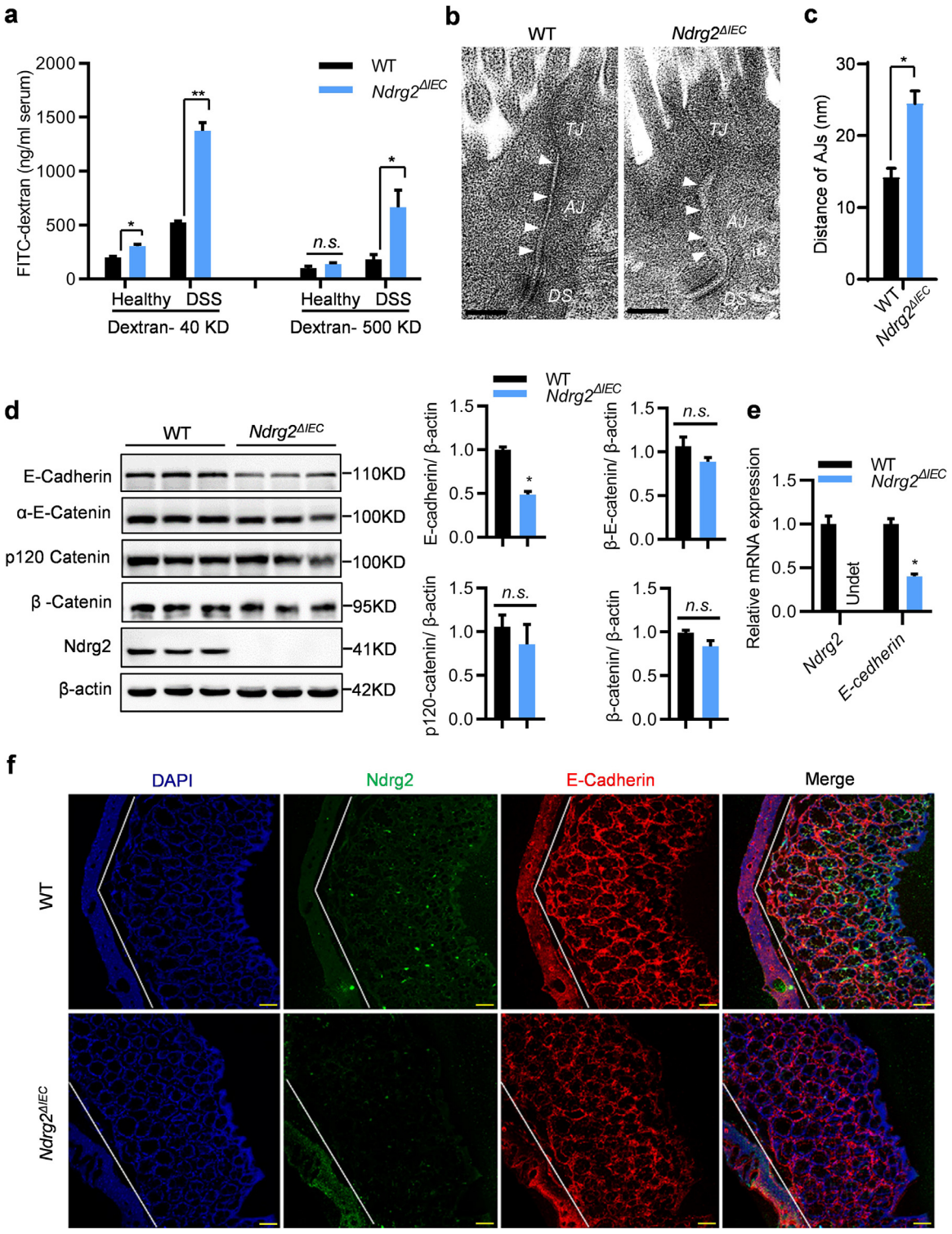

Fig. 4. *Ndrg2* deletion disrupted adherens junctions (AJs) integrity in the colonic epithelium. (a) Intestinal permeability was measured by determining serum FITC-dextran concentrations (40 KD and 500 KD, respectively) (n=8/group). **(b)** AJ structure detection in the colonic epithelium of WT and *Ndrg2*$^{\Delta IEC}$ mice via electron microscopy. Representative image of 6 mice in each group. Bar: 200 nm. **(c)** Quantification of AJ width in the colonic epithelium of WT and *Ndrg2*$^{\Delta IEC}$ mice (n=6/group). **(d)** Western blotting detection of E-Cadherin, α-E-Cadherin, p120 Cadherin, β-Catenin, Snail and Ndrg2 expression in the IECs of WT and *Ndrg2*$^{\Delta IEC}$ mice (left panel, n=3/group), and band intensity quantification in the right panel. **(e)** qRT-PCR analysis of E-cadherin. **(f)** Immunofluorescence micrographs of NDRG2 (green) and E-cadherin (red) expression in the colons of WT and *Ndrg2*$^{\Delta IEC}$ mice (n=6/group). Bar: 100 μm. **(a), (c), (d), (e)** Data are represented as the mean ± SEM. $^{*}p<0.05$, $^{**}p<0.01$, *n.s.*, no significance, (Student's t test). Data are representative of 3 independent experiments.

co-localization of NDRG2 with Snail and FBXO11, respectively (Supplementary Fig. 10). Additionally, as shown by the immunoprecipitation assay in Fig. 5(h), NDRG2/FL could interact with FBXO11 and significantly strengthen FBXO11 targeting to Snail (Fig. 5(i)) to further promote Snail ubiquitination (Fig. 5(j)). Our data demonstrated that NDRG2 could enhance E3 ligase FBXO11 with Snail to induce ubiquitin-mediated degradation of Snail, finally augmenting E-cadherin expression.

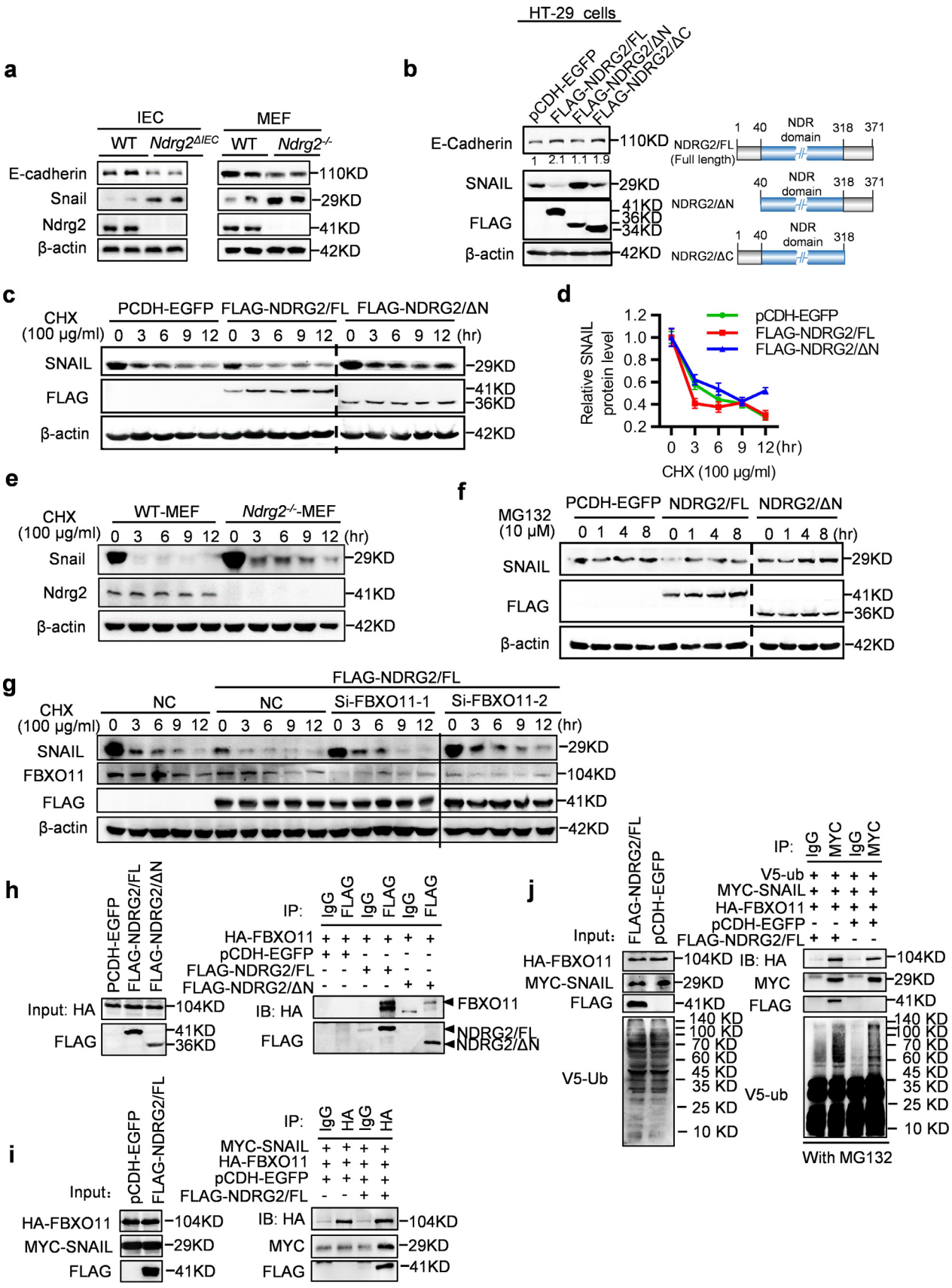

Fig. 5. NDRG2 augmented E-cadherin expression by promoting the ubiquitylation and degradation of SNAIL. (a) Western blot analysis of E-cadherin, Snail and Ndrg2 protein levels in intestinal epithelial cells (IECs) separated from WT and *Ndrg2*$^{\Delta IEC}$ mice (left panel), and in mouse embryonic fibroblast (MEF) cells established from WT and CMV-Cre; *Ndrg2*$^{\Delta IEC}$ mice (right panel). **(b)** Western blotting analysis of endogenous E-Cadherin and SNAIL protein levels in full-length NDRG2 (NDRG2/FL), N-terminal truncation (NDRG2/ΔN) and C-terminal truncation (NDRG2/ΔC) stably overexpressing HT-29 cells (left panel). Graphical representation of NDRG2/FL, NDRG2/ΔN and NDRG2/ΔC truncation mutants (right panel). **(c)** With 100 μg/ml cycloheximide (CHX) treatment, western blot detection of the SNAIL protein half-life in the above-mentioned cells, and quantification in **(d)** using

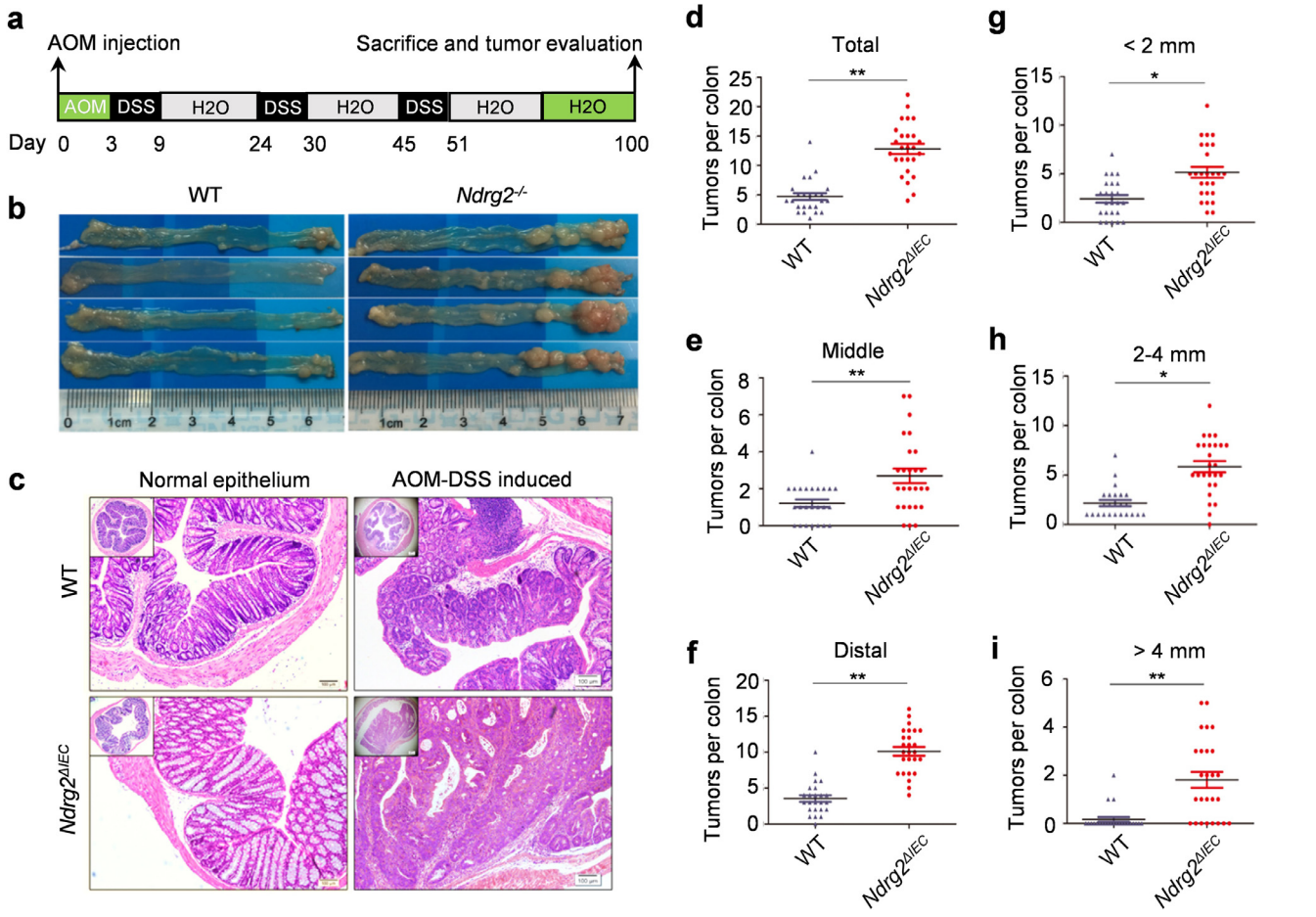

Fig. 6. Intestinal deletion of *Ndrg2* enhanced the initiation and progression of AOM-DSS-induced colorectal carcinoma. **(a)** The method used for the treatment of AOM-DSS in our study. **(b)** Tumour-bearing colon sections from WT and $Ndrg2^{\Delta IEC}$ mice after AOM-DSS treatment. Representative images from WT (n=24) and $Ndrg2^{\Delta IEC}$ (n=26) mice. **(c)** HE staining of normal epithelium and AOM-DSS induced colorectal carcinoma in WT and $Ndrg2^{\Delta IEC}$ mice. Representative images from WT (n=24) and $Ndrg2^{\Delta IEC}$ (n=26) mice. Bar: 100 μm. **(d)**–**(f)** Quantification analysis of tumour numbers from the whole, middle and distal colons of WT and $Ndrg2^{\Delta IEC}$ mice. **(g)**–**(i)** Quantification analysis of tumour numbers with small size (<2 mm), middle size (2–4 mm) and big size (>4 mm) from whole colon of WT and $Ndrg2^{\Delta IEC}$ mice. WT: n=24; $Ndrg2^{\Delta IEC}$: n=26. $^{*}p<0.05$, $^{**}p<0.01$, (Student's t test).

3.6. Ndrg2 loss in intestinal epithelial cells increases colitis-associated colorectal cancer

To further evaluate the role of *Ndrg2* in colitis-associated tumour development, mice were subjected to azoxymethane (AOM) intraperitoneal injection followed by three cycles of the DSS-H_2O rotation treatment (Fig. 6(a)). The mice were then sacrificed, and colon tissues were collected. After the treatment with AOM/DSS, both WT and $Ndrg2^{\Delta IEC}$ mice developed colon tumours mainly in the distal to middle colon, and the $Ndrg2^{\Delta IEC}$ mice showed a dramatic increase in tumour number and size compared with the WT mice (Fig. 6(b)). This phenotype was confirmed by HE staining, as typical cancerization was observed on the distal colon tissue slides (Fig. 6(c)). To further analyse carcinoma formation in WT and $Ndrg2^{\Delta IEC}$ mice, we calculated the distribution, number and size of tumours and observed significant increases in tumours located in the middle and terminal colon (Fig. 6(d), (e), (f)). Moreover, the numbers of tumours with all volume scales (under 2 mm, 2–4 mm and above 4 mm) were increased in $Ndrg2^{\Delta IEC}$ mice (Fig. 6(g), (h), (i)). Our data clearly demonstrated that intestinal *Ndrg2* loss increased susceptibility to colitis-associated tumour development.

3.7. NDRG2 downregulation attenuates E-cadherin expression and enhances inflammation in human IBD patients

To confirm the role of NDRG2 in clinic IBD initiation, we further examined whether NDRG2 affected inflammation in human UC and CD patients (Supplementary Table 3). Interestingly, in UC patients,

ImageJ software. **(e)** Western blotting detection of Ndrg2 and Snail protein levels in MEF cells as mentioned above treated with CHX for the indicated times. **(f)** Endogenous SNAIL protein expression levels in NDRG2/FL and NDRG2/ΔN stably overexpressing HT-29 cells treated with 10 μM MG132 for the indicated time. **(g)** Using CHX (100 μg/ml) treatment and two siRNAs targeting FBXO11 with NC as a negative control, Western blotting analysis of SNAIL, FBXO11 and FLAG-NDRG2 protein expression was performed in parental or FLAG-NDRG2/FL overexpressing SW480 cells. **(h)** HEK293T cells were co-transfected with plasmids expressing HA-FBXO11, FLAG-NDRG2/FL and FLAG-NDRG2/ΔN as indicated, with EGFP as a control. The cell lysate was immunoprecipitated with FLAG antibody or IgG with anti-HA and anti-FLAG as primary antibodies for western blot analysis. **(i)** HEK293T cells were co-transfected with plasmids as indicated. Cell lysates were immunoprecipitated with anti-HA and anti-Myc/FLAG antibodies for western blot analysis. **(j)** HEK293T cells were co-transfected with plasmids expressing HA-FBXO11, Myc-Snail and V5-Ubiquitin together, together with either EGFP or FLAG-NDRG2/FL. Cells were treated with 10 μM MG132 for 6 hrs before the cell lysates were immunoprecipitated with anti-FLAG antibody, and the poly-ubiquitylated Snail protein was detected with anti-V5 antibody. All experiments were repeated at least 3 times independently.

NDRG2 expression was significantly positively correlated with E-cadherin and negatively correlated with Snail (Fig. 7(a)(c)). Most importantly, NDRG2 expression was negatively correlated with inflammation levels and CD68$^+$ macrophage recruitment. Higher NDRG2 expression was correlated with reduced inflammation and CD68$^+$ macrophage recruitment at inflammatory foci, while decreases in NDRG2 expression enhanced inflammation and CD68$^+$ macrophage infiltration (Fig. 7(a), (d), (e)).

Taken together, our findings demonstrated that NDRG2 could positively enhance E-cadherin expression to maintain AJ structure and intestinal epithelial barrier integrity, thus suppressing colonic inflammation. However, intestinal *Ndrg2* loss led to E-cadherin attenuation and AJ structure destruction, resulting in an increase in intestinal epithelial permeability, thus promoting colitis and colitis-associated tumour development (Fig. 8).

4. Discussion

The gastrointestinal tract (GI) is chronically exposed to large numbers of foreign antigens, toxic molecules and microorganisms, and the epithelial barrier makes important contributions to GI health [4,25]. Epithelial barrier dysfunction is believed to contribute to IBD initiation and pathogenesis, mainly by damaging the structure of tight junctions (TJs) and/or adherens junctions (AJs). Previous reports have demonstrated that AJ and TJ disruption is associated with progressive colonic inflammation in human UC and CD due to increased

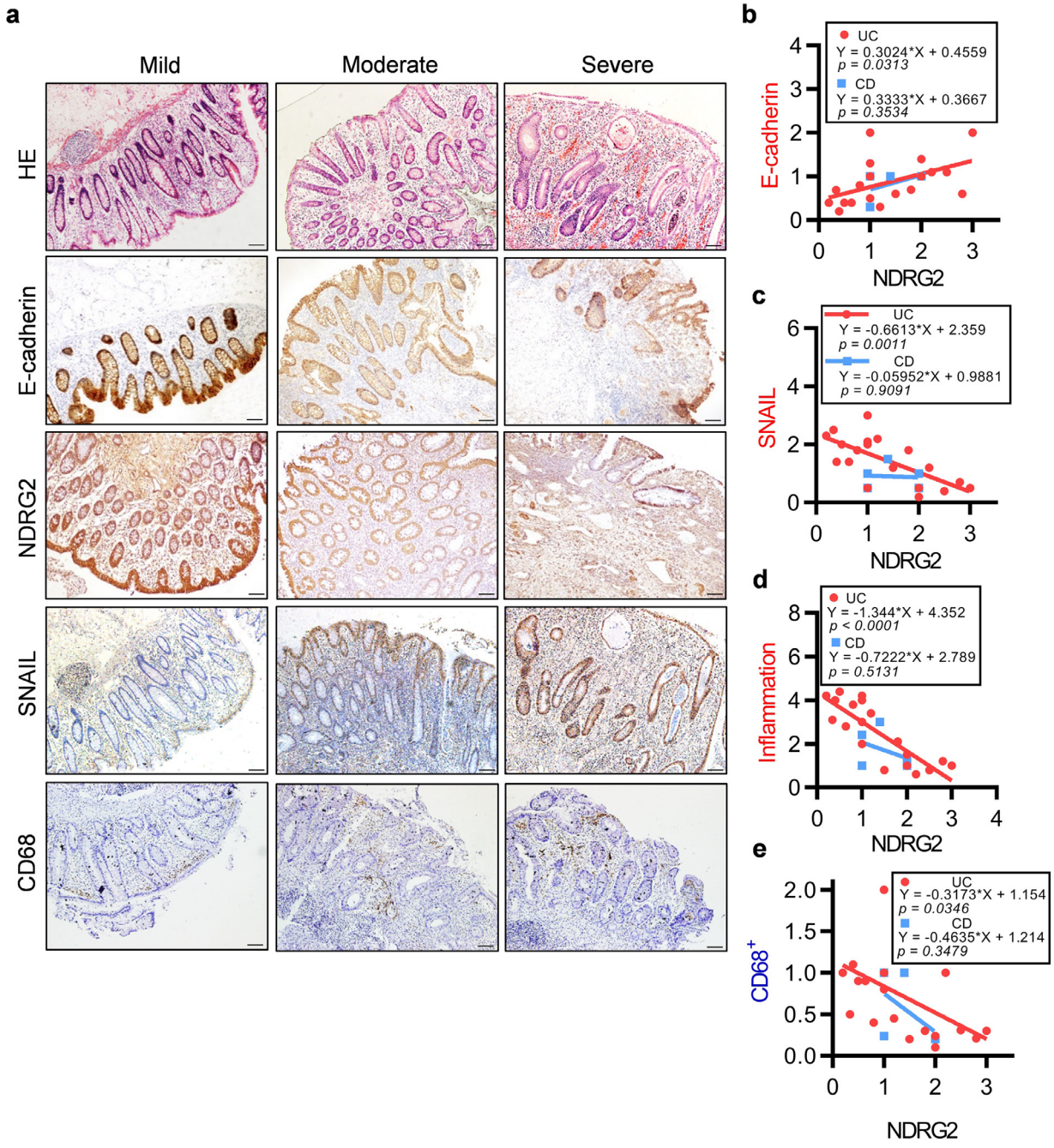

Fig. 7. NDRG2 positively correlated with E-cadherin and negatively correlated with Snail and inflammation in human IBD patients. (a) Immunohistochemistry of NDRG2, E-cadherin, Snail, CD68$^+$ and HE staining of human UC tissues with mild, moderate and severe inflammation. Representative images from UC (n=19) and CD (n=5) patients. Scale bar: 100 μm. **(b)**–**(e)** Linear regression and Pearson's correlation analysis of NDRG2 with inflammation degree, E-cadherin and Snail in UC and CD samples, UC (n=19) and CD (n=5).

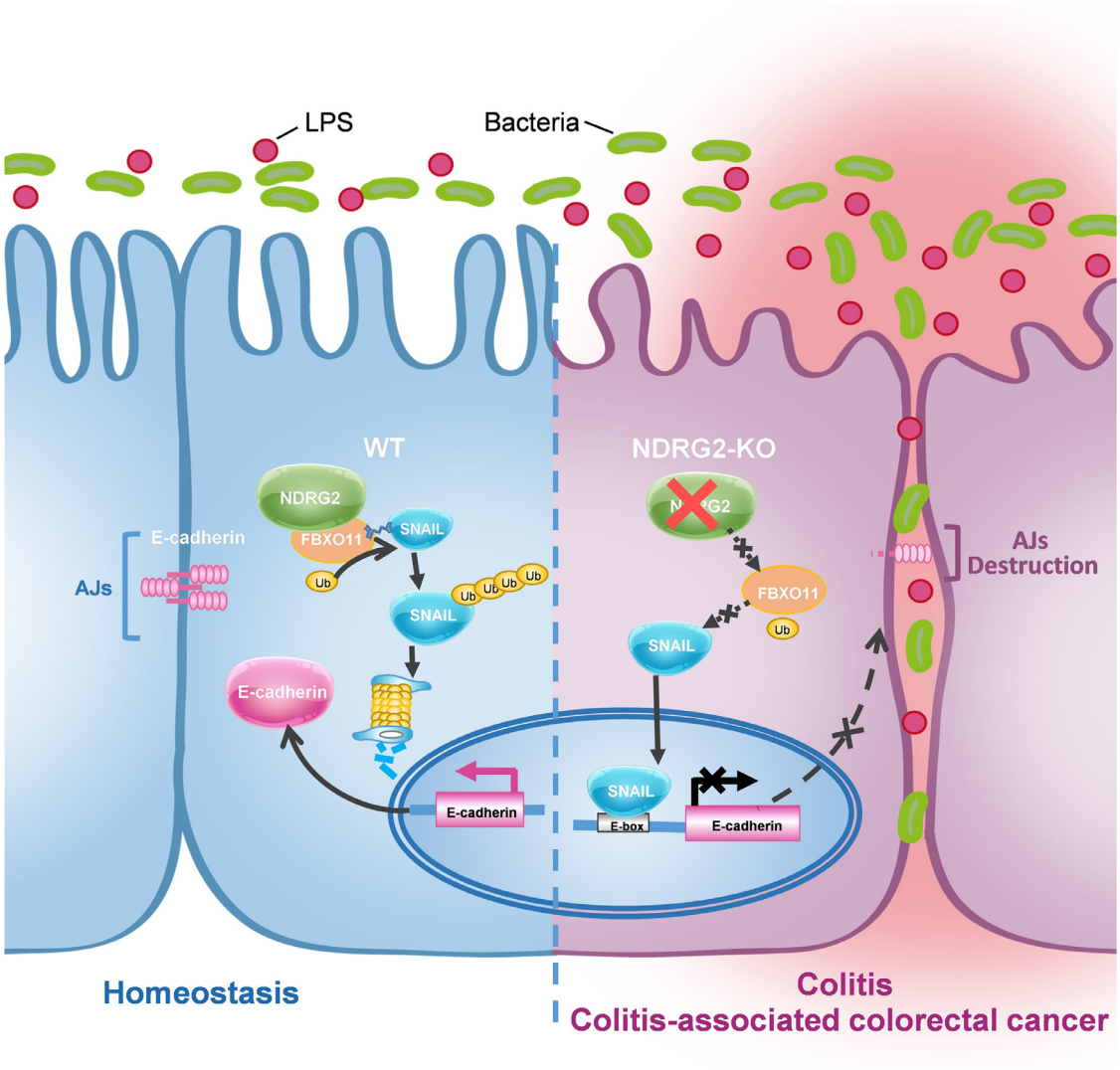

Fig. 8. A schematic for the role of NDRG2 regulating Snail, E-cadherin and adherens junction structural integrity in colitis and colitis-associated tumour development. Intestinal *Ndrg2* loss disrupts the AJ structure in the colonic epithelium by suppressing E-cadherin expression by abrogating Snail ubiquitination and degradation through E3 ligase FBXO11-dependent signalling, thus increasing colonic permeability, colitis and colitis-associated tumour development in *Ndrg2*$^{\Delta IEC}$ mice.

permeability of LPS, peptidoglycan and N-formyl-L-methionyl-L-leucyl-L-phenylalanine (fMLP), which diffuse from the gut lumen to the lamina propria [26,27].

Our study explored the role of NDRG2 in intestinal inflammation pathogenesis and determined that NDRG2 modulated the AJ structure *via* FBXO11/Snail/E-cadherin signalling regulation *in vivo*. NDRG2 was initially discovered and demonstrated to be a tumour suppressor gene by our group. We found that NDRG2 played roles in cancer cell proliferation, differentiation and invasion [28,29]. NDRG2 expression was positively correlated with cancer prognosis and overall survival [10]. Furthermore, NDRG2 regulated EMT by controlling E-cadherin expression and participated in TGF-β-induced oncogenesis in late-stage CRC [30, 31].

E-cadherin is an important cytomembrane component and controls cell-cell adhesion by conjugating to β-catenin, α-catenin and p120-catenin complexes to modulate the spaces between epithelial cells [32,33]. Previous studies have confirmed that reduced E-cadherin aggravates DSS-induced colitis [6,34]. Our work demonstrated that *Ndrg2* loss in intestinal epithelial cells caused AJ destruction but did not disrupt the tight junction structure, as determined *via* electron microscopic analysis. Moreover, we observed obvious reduced E-cadherin expression with no significant alterations of β-catenin or p120-catenin in *Ndrg2*$^{\Delta IEC}$ mice, indicating that AJ destruction caused by *Ndrg2* loss was mainly induced by E-cadherin suppression. Therefore, intestinal *Ndrg2* deletion decreased E-cadherin expression and destroyed the integrity of adherens junctions to increase epithelial barrier permeability, resulting in spontaneous colitis with ageing, and increasing susceptibility to DSS and TNBS-induced colitis. Noticeably, we further found that intestinal *Ndrg2* loss could promote colitis-associated tumour development, which is highly coincident with its tumour suppressor function.

Snail and Slug are believed to be the most important transcriptional repressors of E-cadherin in various types of solid tumours and tissues [35,36]. Our data showed that Snail significantly increased in *Ndrg2*-deficient IECs and MEF cells, suggesting that reduced E-cadherin expression by *Ndrg2* loss might occur mainly through Snail upregulation. Furthermore, we first demonstrated that NDRG2 could strengthen the interaction of E3 ligase FBXO11 with Snail to promote the ubiquitination and degradation of Snail. Thus, as shown in Fig. 4 and 5, intestinal *Ndrg2* deletion disrupted adherens junction structure in the intestinal epithelium by suppressing E-cadherin expression by promoting the FBXO11-Snail interaction for Snail ubiquitination and degradation, thus increasing colonic permeability, colitis and colitis-associated tumour development.

Inflammatory cell infiltration plays an important role in IBD [37], and we found that *Ndrg2* loss facilitated inflammatory cell

recruitment and that reduced NDRG2 expression was associated with the severe inflammatory state in clinical samples of UC patients. Most importantly, we confirmed the positive correlation of NDRG2 with E-cadherin and the negative correlation with Snail in UC samples. However, it was difficult to recognize this similar pattern in CD patients, partially due to the limited CD patient samples, which might also suggest the different function of NDRG2 in UC and CD. *Ndrg2* loss-induced E-cadherin repression leads to an increase in intestinal permeability and pro-inflammatory cytokine production, thereby triggering a greater immune response to further aggravate colitis progression.

In summary, our work confirmed that NDRG2 played an important role in colitis initiation and pathogenesis by enhancing E-cadherin expression and regulating AJ structural integrity to maintain gut homeostasis. However, intestinal *Ndrg2* deficiency resulted in attenuated E-cadherin expression and AJ structure disruption, finally promoting colitis and colitis-associated tumour development (Fig. 8). Thus, NDRG2 might be an important diagnostic and prognostic marker of colitis and colitis-associated colorectal cancer.

Contributors

Design of studies: JZ, JPL, LBY and KCW. Performance of the mice husbandry, DSS, AOM/DSS animal model and phenotyping: MYW, YZM, LLS. performed of the intestinal gene expression analysis and tissue dissection: YQX, ZHG, LJL, XB, HYQ. Clinical assessments: YQX, ZSL, ZW. Writing of the manuscript: JZ, MYW, YZM. All authors approved the manuscript.

Data sharing statement

Data are available upon request.

Declaration of Competing Interest

The authors declare no competing interests.

Acknowledgments

We are thankful for the critical discussion and technical support from Professor Jing Ye.

Supplementary materials

Supplementary material associated with this article can be found, in the online version, at doi:10.1016/j.ebiom.2020.103068.

References

[1] de Souza H S P, Fiocchi C, Iliopoulos D. The IBD interactome: an integrated view of aetiology, pathogenesis and therapy. Nat Rev Gastroenterol Hepatol 2017;14(12):739–49.
[2] Arrieta M C, Bistritz L, Meddings J B. Alterations in intestinal permeability. Gut 2006;55(10):1512–20.
[3] Stein J, Ries J, Barrett K E. Disruption of intestinal barrier function associated with experimental colitis: possible role of mast cells. Am J Physiol 1998;274(1 Pt 1):G203–9.
[4] Taddei A, Giampietro C, Conti A, Orsenigo F, Breviario F, Pirazzoli V, et al. Endothelial adherens junctions control tight junctions by VE-cadherin-mediated upregulation of claudin-5. Nat Cell Biol 2008;10(8):923–34.
[5] Smalley-Freed W G, Efimov A, Burnett P E, Short S P, Davis M A, Gumucio D L, et al. p120-catenin is essential for maintenance of barrier function and intestinal homeostasis in mice. J Clin Investig 2010;120(6):1824–35.
[6] Grill J I, Neumann J, Hiltwein F, Kolligs F T, Schneider M R. Intestinal E-cadherin deficiency aggravates dextran sodium sulfate-induced colitis. Digest Dis Sci 2015;60(4):895–902.
[7] Ha S D, Ng D, Pelech S L, Kim S O. Critical role of the phosphatidylinositol 3-kinase/Akt/glycogen synthase kinase-3 signaling pathway in recovery from anthrax lethal toxin-induced cell cycle arrest and MEK cleavage in macrophages. J Biol Chem 2007;282(50):36230–9.
[8] Rembutsu M, Soutar M P, Van Aalten L, Gourlay R, Hastie C J, McLauchlan H, et al. Novel procedure to investigate the effect of phosphorylation on protein complex formation in vitro and in cells. Biochemistry 2008;47(7):2153–61.
[9] Shen L, Qu X, Li H, Xu C, Wei M, Wang Q, et al. NDRG2 facilitates colorectal cancer differentiation through the regulation of Skp2-p21/p27 axis. Oncogene 2018.
[10] Chu D, Zhang Z, Li Y, Wu L, Zhang J, Wang W, et al. Prediction of colorectal cancer relapse and prognosis by tissue mRNA levels of NDRG2. Mol Cancer Ther 2011;10(1):47–56.
[11] Harris E S, Nelson W J. Adenomatous polyposis coli regulates endothelial cell migration independent of roles in beta-catenin signaling and cell-cell adhesion. Mol Biol Cell 2010;21(15):2611–23.
[12] Han J, Lin H, Huang W. Modulating gut microbiota as an anti-diabetic mechanism of berberine. Med Sci Monit: Int Med J Exp Clin Res 2011;17(7):Ra164–7.
[13] Membrez M, Blancher F, Jaquet M, Bibiloni R, Cani P D, Burcelin R G, et al. Gut microbiota modulation with norfloxacin and ampicillin enhances glucose tolerance in mice. FASEB J: Off Publ Feder Am Soc Exp Biol 2008;22(7):2416–26.
[14] Huang B, Chen Z, Geng L, Wang J, Liang H, Cao Y, et al. Mucosal profiling of pediatric-onset colitis and IBD reveals common pathogenics and therapeutic pathways. Cell 2019;179(5):1160–76 e1124.
[15] Pastorelli L, Dozio E, Pisani L F, Boscolo-Anzoletti M, Vianello E, Munizio N, et al. Procoagulatory state in inflammatory bowel diseases is promoted by impaired intestinal barrier function. Gastroenterol Res Pract 2015;2015:189341.
[16] Mohanan V, Nakata T, Desch AN, Levesque C, Boroughs A, Guzman G, et al. C1orf106 is a colitis risk gene that regulates stability of epithelial adherens junctions. Science 2018;359(6380):1161–6.
[17] Li J N, Li X, Qian J M, Lu X Q, Yang H. Effects of K-ras gene mutation on colon cancer cell line Caco-2 metastasis by regulating E-cadherin/beta-catenin/p120 protein complex formation and RhoA protein activity. Zhongguo Yi Xue Ke Xue Yuan Xue Bao 2010;32(1):46–50.
[18] Hartsock A, Nelson W J. Adherens and tight junctions: structure, function and connections to the actin cytoskeleton. Biochim Biophys Acta 2008;1778(3):660–9.
[19] Li Y, Yin A, Sun X, Zhang M, Zhang J, Wang P, et al. Deficiency of tumor suppressor NDRG2 leads to attention deficit and hyperactive behavior. J Clin Investig 2017.
[20] Nakahata S, Ichikawa T, Maneesaay P, Saito Y, Nagai K, Tamura T, et al. Loss of NDRG2 expression activates PI3K-AKT signalling via PTEN phosphorylation in ATLL and other cancers. Nat Commun 2014;5:3393.
[21] Wang Y, Shi J, Chai K, Ying X, Zhou B P. The role of snail in EMT and tumorigenesis. Curr Cancer Drug Targets 2013;13(9):963–72.
[22] Krebs A M, Mitschke J, Lasierra Losada M, Schmalhofer O, Boerries M, Busch H, et al. The EMT-activator Zeb1 is a key factor for cell plasticity and promotes metastasis in pancreatic cancer. Nat Cell Biol 2017;19(5):518–29.
[23] Diaz V M, de Herreros A G. F-box proteins: keeping the epithelial-to-mesenchymal transition (EMT) in check. Semin Cancer Biol 2016;36:71–9.
[24] Zheng H, Shen M, Zha Y L, Li W, Wei Y, Blanco M A, et al. PKD1 phosphorylation-dependent degradation of SNAIL by SCF-FBXO11 regulates epithelial-mesenchymal transition and metastasis. Cancer Cell 2014;26(3):358–73.
[25] Peterson L W, Artis D. Intestinal epithelial cells: regulators of barrier function and immune homeostasis. Nat Rev Immunol 2014;14(3):141–53.
[26] Landy J, Ronde E, English N, Clark S K, Hart A L, Knight S C, et al. Tight junctions in inflammatory bowel diseases and inflammatory bowel disease associated colorectal cancer. World J Gastroenterol 2016;22(11):3117–26.
[27] Kobayashi K, Oyama S, Numata A, Rahman M M, Kumura H. Lipopolysaccharide disrupts the milk-blood barrier by modulating claudins in mammary alveolar tight junctions. PloS One 2013;8(4):e62187.
[28] Yao L, Zhang J, Liu X. NDRG2: a Myc-repressed gene involved in cancer and cell stress. Acta Biochim Biophys Sin 2008;40(7):625–35.
[29] Li M, Lai X, Zhao Y, Zhang Y, Li M, Li D, et al. Loss of NDRG2 in liver microenvironment inhibits cancer liver metastasis by regulating tumor associate macrophages polarization. Cell Death Dis 2018;9(2):248.
[30] Shen L, Qu X, Ma Y, Zheng J, Chu D, Liu B, et al. Tumor suppressor NDRG2 tips the balance of oncogenic TGF-beta via EMT inhibition in colorectal cancer. Oncogenesis 2014;3:e86.
[31] Kim Y J, Kang H B, Yim H S, Kim J H, Kim J W. NDRG2 positively regulates E-cadherin expression and prolongs overall survival in colon cancer patients. Oncol Rep 2013;30(4):1890–8.
[32] Bulgakova N A, Brown N H. Drosophila p120-catenin is crucial for endocytosis of the dynamic E-cadherin-Bazooka complex. J Cell Sci 2016;129(3):477–82.
[33] Orsulic S, Huber O, Aberle H, Arnold S, Kemler R. E-cadherin binding prevents beta-catenin nuclear localization and beta-catenin/LEF-1-mediated transactivation. J Cell Sci 1999;112(Pt 8):1237–45.
[34] Wheeler J M, Kim H C, Efstathiou J A, Ilyas M, Mortensen N J, Bodmer W F. Hypermethylation of the promoter region of the E-cadherin gene (CDH1) in sporadic and ulcerative colitis associated colorectal cancer. Gut 2001;48(3):367–71.
[35] Yokoyama K, Kamata N, Hayashi E, Hoteiya T, Ueda N, Fujimoto R, et al. Reverse correlation of E-cadherin and snail expression in oral squamous cell carcinoma cells in vitro. Oral oncology 2001;37(1):65–71.
[36] Hajra K M, Chen D Y, Fearon E R. The SLUG zinc-finger protein represses E-cadherin in breast cancer. Cancer Res 2002;62(6):1613–8.
[37] Montagna E, Cancello G, Torrisi R, Rizzo S, Scarano E, Colleoni M. Lapatinib and metronomic capecitabine combination in an HER2-positive inflammatory breast cancer patient: a case report. Ann Oncol 2010;21(3):667–8.